American Mineralogist, Volume 78, pages 657–664, 1993

An adaptation of the spindle stage for geometric analysis of fluid inclusions

ALAN J. ANDERSON, ROBERT J. BODNAR
Fluids Research Laboratory, Department of Geological Sciences, Virginia Polytechnic Institute and State University, Blacksburg, Virginia 24061, U.S.A.

ABSTRACT

In order to view fluid inclusions in three dimensions, a spindle stage has been modified to accommodate large mineral grains and doubly polished sections prepared for fluid inclusion analysis. With the spindle stage technique, fluid inclusions within a grain can be observed under the microscope as they are rotated 360° about either a horizontal (spindle) or vertical (microscope stage) axis. Three-dimensional observation of samples with fluid inclusions affords more accurate measurement of (1) the dimensions of individual fluid inclusions and their contained phases, (2) the depth of fluid inclusions below the polished surface of the host mineral, and (3) the angular relationship between planar arrays of fluid inclusions with respect to optical and crystallographic directions in the host crystal or to structural features in the host rock. These measurements have been difficult or impossible to obtain using conventional petrographic methods.

Application of this spindle stage technique will eliminate many of the uncertainties concerning the origin of inclusion trails and their relationship to structural or crystallographic features in the samples being examined. Use of this method in conjunction with microanalytical techniques that require knowledge of the physical characteristics of the inclusion, such as thickness and volume of the inclusion and its depth below the surface, will improve the accuracy obtained with these techniques. Moreover, the spindle stage is a relatively inexpensive alternative to the universal stage and offers a greater degree of rotation about the horizontal axis.

INTRODUCTION

The study of fluid inclusions consists of (1) an initial petrographic examination of the inclusions, followed by (2) microthermometric and microchemical analysis and data interpretation. During the past several decades, significant advances in data measurement and interpretation techniques have been made as new instrumentation for microthermometric and chemical analysis have become available (see, for example, Roedder, 1991) and *PVTX* data for the appropriate fluid systems have been obtained over a wide range of physical and chemical conditions. Conversely, techniques for mapping the distribution of inclusions within a sample and for determining the geometry of individual inclusions have progressed little during the past century. These parameters are most often based on the characteristics of inclusions as observed in two dimensions within a fixed plane. The orientation of planar and linear arrays of fluid inclusions with respect to crystallographic directions in the host mineral is the most important characteristic for determining the temporal classification of inclusions (Roedder, 1984). Additionally, knowledge of the orientation of inclusion planes relative to macrostructural features in the host rock is necessary to understand the timing of various fluid events with respect to the tectonic and deformational history of the rock. Finally, the size and shape of individual fluid inclusions and their contained phases must be known for many applications, and this information can often be only poorly approximated from two-dimensional observation. At the present time, the inability to accurately define the geometric characteristics of groups of inclusions and individual inclusions is the single most important obstacle, and results in a great deal of the uncertainty, in fluid inclusion studies.

Tuttle (1949) and numerous subsequent workers used the universal stage to measure the geometry of fluid inclusion planes in oriented sections, but the geometric limitations of the universal stage preclude measurement of planes dipping $<45°$ in a given section. An alternative approach employed by Boullier and Robert (1992) facilitated measurements of both steep- and shallow-dipping microcracks by measuring the thickness of each mineral plate with a calibrated micrometric focusing screw and then converting the projected width of an inclusion plane into its dip. This method represents a significant improvement over commonly used two-dimensional observations in a fixed plane, but it is very tedious and time consuming and lacks the precision of the universal stage, particularly for measurements of the most shallowly dipping planes. In order to optimize the precision of their measurements, Boullier and Robert examined two or three orthogonal fluid inclusion plates from each sample.

Three-dimensional imaging of fluid inclusions using

0003–004X/93/0506–0657$02.00

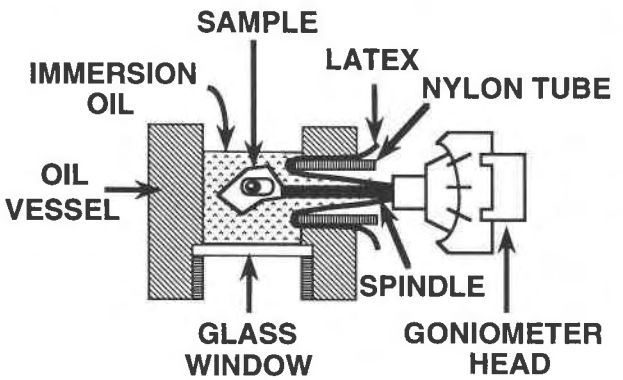

Fig. 1. Schematic illustration of the modified oil immersion vessel for the spindle stage.

confocal scanning laser microscopy was recently suggested by Petford and Miller (1992). Confocal three-dimensional images are achieved by compiling serial sections through the sample with the aid of image analysis software. This new technique is potentially useful for inclusion petrography, but the high instrumentation cost may limit its application in many laboratories currently involved in fluid inclusion studies.

In this paper we describe the design, operation, and application of a new adaptation of the spindle stage (Wilcox, 1959) for geometric analysis of fluid inclusions. This relatively inexpensive tool (<$700.00 U.S.) can be used to define the orientation of planar and linear features in translucent minerals, as well as to determine the shape and size of individual fluid inclusions.

Modifications and operation of the spindle stage

The spindle stage (Wilcox, 1959; Bloss, 1981) is a simple yet powerful tool used to measure the optical constants of anisotropic crystals by immersion techniques. With the spindle stage, a crystal can be rotated 360° about either a vertical (microscope stage) or horizontal (spindle) axis, so that any desired linear feature in the crystal may be rotated into the plane of the microscope stage, thus allowing all three principal indices to be directly determined from the same grain (Bloss, 1981). Similarly, any planar feature can be rotated about a horizontal axis until it is in the vertical plane, allowing the orientation of the feature with respect to some other feature (crystallographic axis or external feature) to be determined.

For optical studies it is preferable to use crystals that are typically <1 mm in diameter. Hence, conventional spindle stages are equipped with a shallow immersion cell that is sufficient to completely bathe a tiny crystal in oil. In contrast, samples examined in fluid inclusions studies are considerably larger in most cases, and so a special oil immersion vessel was designed to accommodate larger samples (up to 1 cm in diameter).

Figure 1 is a schematic representation of the modified oil immersion vessel. The vessel is machined out of Al.

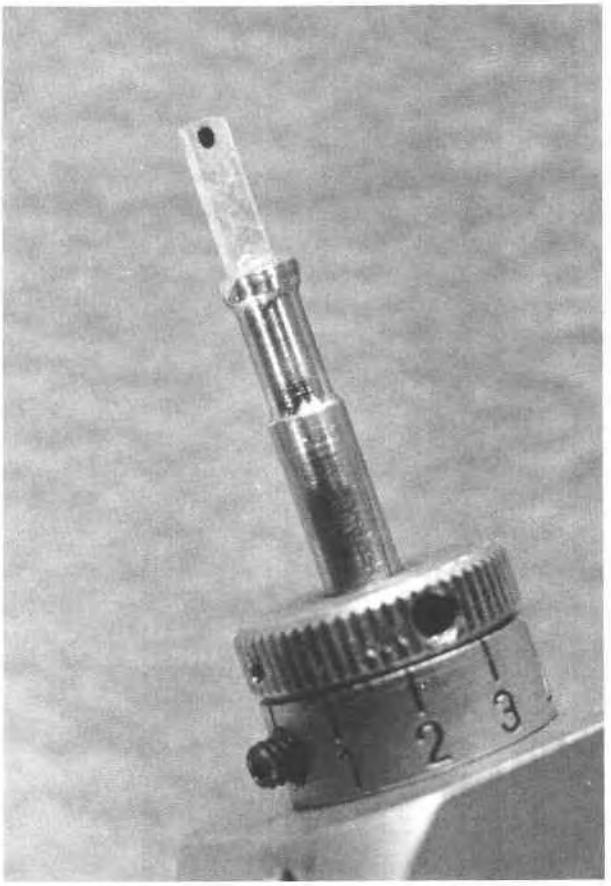

Fig. 2. Photograph of a doubly polished rectangular prism of quartz mounted on the end of an Al spindle. The dot on the surface designates the upper horizontal surface, and the long dimension of the prism is parallel to a reference azimuth.

An optical glass window serves as the bottom of the vessel. The spindle is 24 mm in length, which is about twice the length of the specimen mount pins normally used for single-crystal X-ray diffraction studies. The latex film, which separates the spindle from the goniometer head, prevents the immersion oil from leaking out of the vessel and also provides the flexibility required to orient a given inclusion with the goniometer head. Standard immersion oil will dissolve latex; therefore it is necessary to use a refractive index oil that is compatible with latex, such as Cargille Laser Liquid.

The oil immersion cell shown in Figure 1 can accommodate samples as large as 1 cm in diameter, but in practice the maximum sample size depends on the clarity of the sample. Mineral grains or portions of doubly polished plates are attached to the end of an Al spindle with cyanoacrylic cement. Those spindles intended to hold doubly polished plates have a slot cut into one end where the plate is to be inserted. For the analysis of microcracks, oriented samples are sectioned and cut into rectangular prisms where the long dimension of the prism is cut parallel to a reference azimuth and the upper surface is

marked with a dot. The rectangular prisms were typically cut to a dimension of ca. 7 × 2 × 1 mm and mounted on an Al spindle (Fig. 2).

Once the sample is securely mounted, the opposite end of the spindle is pressed into the latex and inserted into the goniometer head. The latex, which envelops the spindle, is threaded through a nylon tube and folded back over its outer surface, until the tube is completely surrounded. The sample is then positioned in the vessel through a side port as the tube is pressed into the port. Immersion oil with a refractive index that matches a principal index of the host mineral is added to the vessel with a pipette until the mineral is totally immersed. The level of immersion liquid in the vessel must be well above the spindle so that the mounted sample remains totally submerged throughout its rotation. A circular glass cover slide can be placed on the top of the vessel to contain the fumes from the immersion liquid. Microscope objectives with a long working distance must be used to view the sample within the oil vessel, and a long working-length substage condenser is also recommended for optimum optics.

With the spindle stage the orientation of any planar or linear feature can be precisely measured with respect to a reference direction. The reference direction may be (1) an optical constant derived from extinction measurements, (2) a crystallographic feature such as a cleavage plane, growth zone, crystal face (positive or negative), or a twin plane, (3) a micro- or macrostructural feature in the host mineral, or (4) an azimuth and horizontal surface marked on an oriented sample taken from the field. Determination of optical directions in a crystal is facilitated by the computer program EXCALBR II (Bartlemehs et al., 1992). If a quartz crystal exhibits strained extinction, an alternative method (see Bloss, 1981) may be necessary to determine its crystallographic orientation.

Figure 3 illustrates the procedure used to determine the pole to a planar feature. First, a planar array of inclusions, dipping at some unknown angle in the mounted sample, is selected. The plane is then rotated about the horizontal axis until it becomes vertical. The vertical orientation of a planar feature may be checked by focusing through the sample to see if the position of the plane shifts in a lateral sense. Finally, the plane is rotated about the axis of the microscope stage until it is oriented parallel to the north-south cross hair of the eyepiece. The pole to the plane can then be measured, relative to a starting reference position, by the amount of rotation about the horizontal and vertical axes as indicated on the graduations around the edge of the spindle drum and microscope stage, respectively.

To determine a lineation direction, a linear feature within the crystal is rotated about the horizontal axis into the plane of the microscope stage; it is then rotated about the vertical axis to an east-west direction. The amount of rotation about each axis with respect to a reference position is then recorded and plotted on a stereonet.

The spindle stage may also be used to measure the size and shape of an individual fluid inclusion. By rotating a fluid inclusion about the spindle axis, its dimensions can be measured from observation in two mutually perpendicular directions. These dimensions can then be measured using a graduated ocular or a calibrated image analysis system. Figure 4A is a photomicrograph of three solid-liquid-vapor fluid inclusions (a, b, and c) in a grain of quartz from the Bingham Canyon porphyry Cu deposit in Utah. The view in Figure 4A is normal to the c axis of the quartz grain. Figure 4B reveals the same three fluid inclusions after rotation by 90° about the spindle axis. Examination of these negative crystal-shaped inclusions in two orthogonal directions indicates that they are tabular as a result of unequal development of equivalent faces. Three-dimensional viewing of fluid inclusions such as those shown in Figure 4A affords a more accurate measurement of the volume of an inclusion and its contained phases than was previously possible.

The distance between a given inclusion and some other inclusion or feature in the sample may also be easily determined with the spindle stage. For example, the depth of an inclusion below the surface of the host mineral can be directly measured once the polished surface of the mineral plate has been rotated into a vertical position (Fig. 5). By viewing the sample parallel to the polished surface, one can readily locate shallow fluid inclusions that are suitable for in situ microanalysis. For these measurements, it is useful to view the sample with the nicols crossed to clearly define the interface between the mineral and an immersion oil of the matching refractive index.

Applications

The ability to determine the geometric features of fluid inclusion planes or individual inclusions has application to many important fluid inclusion problems. A brief summary of some of these applications and examples of the use of the spindle stage are presented below. The three-dimensional observation afforded by the spindle stage technique is obviously not limited to fluid inclusion studies but is also ideally suited to other studies involving microscopic observation in which the orientation of the feature being observed is important. These studies include, among others, microstructural analysis of deformed materials and fission track measurements.

Identification of primary fluid inclusions

The assignment of inclusion origin is the single most critical stage in the study of natural fluid inclusions (Roedder, 1984). The empirical criteria used to identify inclusions of primary and secondary origin are based to a large extent on the distribution and orientation of inclusions with respect to crystallographic directions of the host mineral and on the size and shape of the inclusions. Relating an inclusion or group of inclusions to a crystallographic direction in the host mineral is difficult, particularly when the host mineral does not display visible zoning. With the spindle stage, the angular relations between a crystallographic direction in the host crystal and arrays

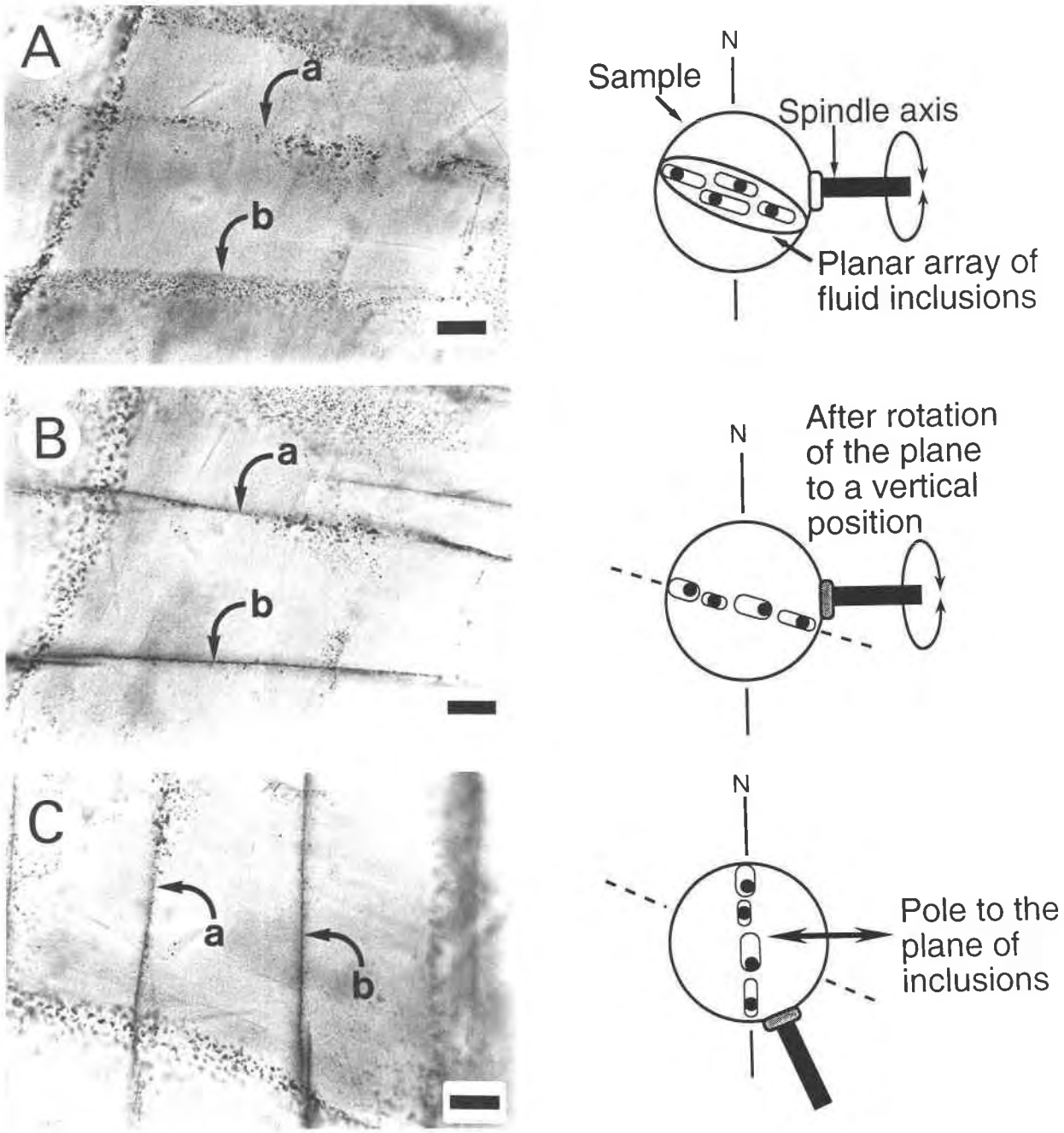

Fig. 3. Serial photographs with companion schematic illustrations depicting the steps involved in determining the pole to a plane of fluid inclusions with the spindle stage. (**A**) Planar arrays of inclusions (a and b) as observed at the starting reference position. (**B**) Same planes after rotation about the horizontal axis such that planes a and b have a vertical orientation. (**C**) Same planes after rotation about the vertical axis such that from the pole to plane b is from east to west. The scale bar represents 100 μm.

of fluid inclusions can be precisely and easily determined. If planes of fluid inclusions are not consistently parallel to prominent crystal directions, then it can be assumed that they are not primary fluid inclusions. The reverse, however, is not true; that is, fluid inclusions that occur along crystal growth directions are not always primary (Roedder, 1984).

The most convincing evidence that a given group of fluid inclusions is primary is if the inclusions are restricted to a growth face in the host mineral. In the case of a mineral such as quartz, which usually does not exhibit visible zoning, the angular relationship between optical constants and a planar array of fluid inclusions may be used to determine whether the inclusions were trapped

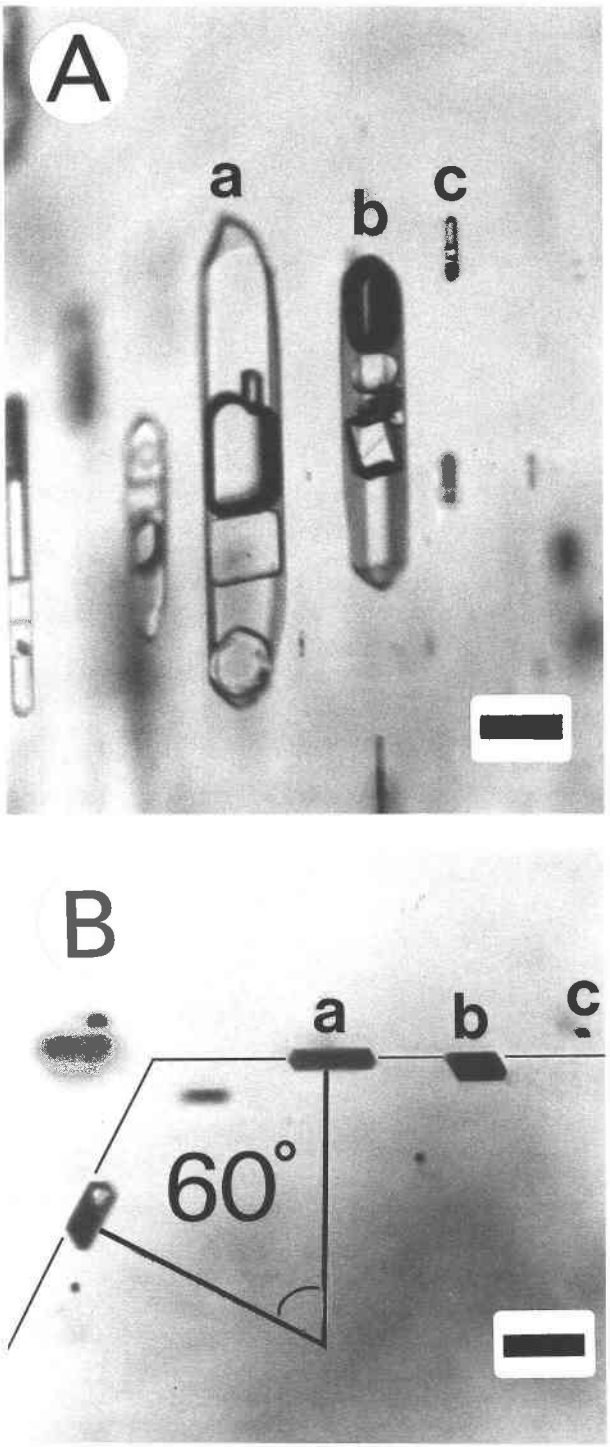

Fig. 4. Photomicrographs of negative crystal-shaped fluid inclusions in quartz, as viewed with the spindle stage; normal to the c axis (**A**), and parallel to the c axis (**B**). Note the tabular shape of the fluid inclusions. The scale bar represents 25 μm.

on a growth surface. Although low quartz displays numerous crystal forms (Frondel, 1962), trapping is most likely to occur on one or more of the five dominant form faces, which are illustrated in Figure 6. Thus, if the inclusions can be consistently related to the faces of one or more of these forms, one can claim with confidence that the inclusions are primary. Planes of secondary inclusions in quartz can occur along cleavages that are parallel to the rhombic faces (Bloss and Gibbs, 1963), but these can usually be distinguished by their undulatory form. With the spindle stage, it is possible to determine not only if the inclusions occur along a growth surface, but also the crystal face on which trapping occurred. For example, Figure 7A depicts two bands of irregularly shaped fluid inclusions in quartz from Collegeville, Pennsylvania, as observed in the polished section cut from the crystal. Figure 7B shows the same bands of inclusions after rotation to a vertical position. The angle between the c axis of the quartz and the plane of fluid inclusions is 38°, and the measured angle between the poles to the fluid inclusion planes is 46°. These angles correspond to the angle between the c axis and the rhombic faces of the host quartz (38°12′32″) and the interfacial angle between the rhombic $\{10\bar{1}1\}$ and $\{01\bar{1}1\}$ form faces (46°15′58″), respectively. In contrast, the plane of fluid inclusions in the quartz vein from the Bingham Canyon mine (Fig. 4B) is oriented with its pole exactly 90° to the c axis of the host crystal and is thus parallel to a prism $\{hki\bar{0}\}$ face of the host quartz.

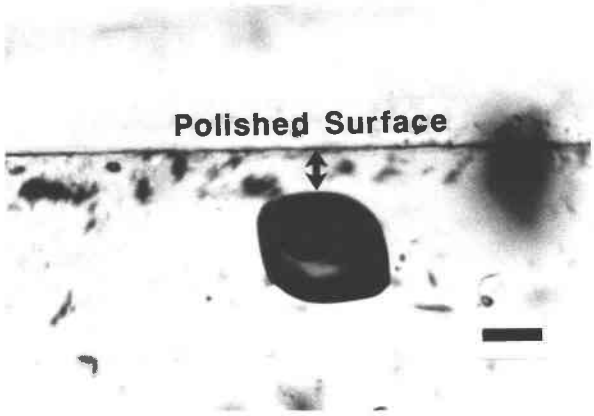

Fig. 5. Photomicrograph of a fluid inclusion in quartz as viewed parallel to the polished surface. The inclusion is 21 μm below the surface. The scale bar represents 25 μm.

Fluid inclusion phase ratios

Constant phase ratios in fluid inclusions is commonly cited as evidence for entrapment of a homogeneous fluid within a narrow range of temperature and pressure. Moreover, consistent phase ratios and microthermometric behavior among a group of inclusions is strong evidence that the inclusions have not leaked or reequilibrated following entrapment. Conversely, the presence of coexisting vapor- and liquid-rich fluid inclusions, or inclusions with a range of liquid to vapor ratios, provides evidence for immiscibility at the time of trapping or later leakage or necking. Bodnar et al. (1985) have demonstrated the unreliability of visual estimates of inclusion phase ratios from observation in two dimensions and have recommended that two-dimensional evidence for immisci-

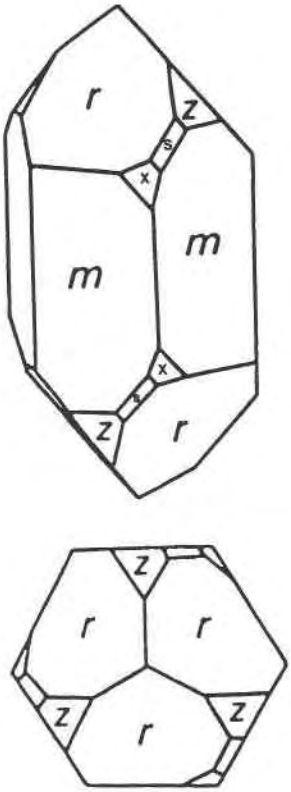

Fig. 6. A crystal of right-low quartz (adapted from Nicolas and Poirier, 1976, their Fig. 5.26), displaying five of the most common forms of low quartz: hexagonal prism (m); positive rhombohedron (r); negative rhombohedron (z); trigonal dipyramid (s); positive trapezohedron (x).

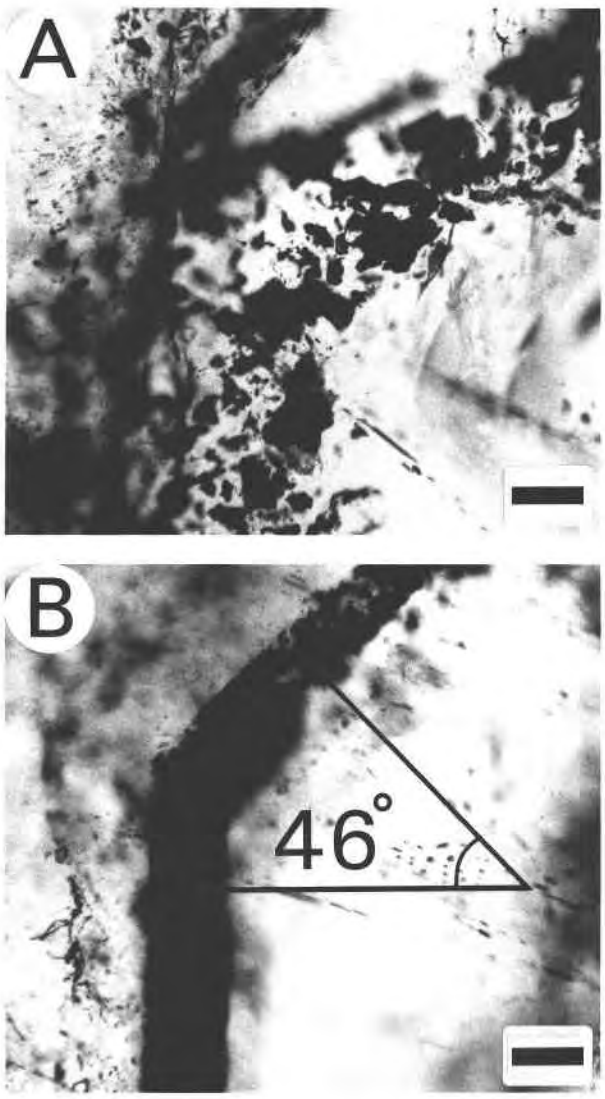

Fig. 7. Planes of irregularly shaped fluid inclusions in quartz (**A**), and after rotation of the same planes of fluid inclusions to a vertical position (**B**). The measured angle between the inclusion planes is 46°. The scale bar represents 100 μm.

bility be confirmed by microthermometric analysis. However, with many fluid inclusions containing high gas contents or insoluble solid phases, decrepitation occurs before homogenization is obtained. Thus, evidence for coexisting liquid- and vapor-rich inclusions may be obtained more reliably using estimates of fluid inclusion phase ratios from observations in two mutually perpendicular directions (Fig. 4) with the spindle stage.

Paleo-fracture analysis

Numerous studies have shown that the orientation of fluid-healed fractures is a valuable paleostress indicator (e.g., Boullier and Robert, 1991, 1992; Lacazette, 1992; Laubach, 1989; Ren et al., 1989). Moreover, the angular relationship between planar arrays of secondary inclusions and micro- and macrostructural features in the host rock can be used to correlate inclusion-decorated microcracks to specific deformational or mineralization events (e.g., Boiron et al., 1992). For example, Kesler (1990) suggested that the study of fluid inclusions with proven association with Au deposition is an important research direction for improving our understanding of the nature and timing of mineralizing solutions in greenstone Au deposits.

Knowledge of the morphology, orientation, and density of annealed cracks in minerals is important to understanding paleo-permeability of a rock and how it evolved with time (Brantley et al., 1990; Smith and Evans, 1984). Lespinasse and Pecher (1986) and Lespinasse et al. (1992) have demonstrated that fluid inclusion orientation analysis is useful for reconstructing the geometry of fluid migration. Furthermore, precise measurements of the morphology of inclusions within annealed cracks will be useful for estimating inclusion formation conditions (Bodnar et al., 1985).

Quantitative microanalysis of individual fluid inclusions.

In situ analysis of single fluid inclusions by proton-induced X-ray emission (PIXE) or synchrotron X-ray fluorescence (SXRF) requires accurate measurement of the

size of the fluid inclusion and its depth beneath the polished surface (Frantz et al., 1988; Anderson et al., 1989). Estimates of these parameters from observation in two dimensions can result in significant error in the calculated X-ray yields. In previous studies (e.g., Anderson et al., 1989) the approximate depth of the inclusion was determined with a petrographic microscope by the vertical displacement of the objective lens from the focused image of the polished surface to that of the fluid inclusion. The minimum and maximum depths of the inclusion extremities, however, cannot be reliably determined using this technique.

In an attempt to measure the size and depth of inclusions in quartz for quantitative PIXE analysis, Ryan et al. (1991) selected only euhedral negative crystals for analysis on the assumption that the unmeasured third dimension of the inclusion (i.e., inclusion thickness) is equal to its minor diameter, as measured from observation normal to the polished surface of the sample. The depth of an inclusion was then determined by measuring to its midplane with a petrographic microscope and then subtracting one-half of the estimated inclusion thickness. In many cases, however, the dimensions of euhedral negative crystal-shaped fluid inclusions deviate significantly from the ideal form because of the unequal development of equivalent faces. For example, by measuring the dimensions of the negative crystal-shaped inclusions in Figure 4A and 4B, it can be seen that the minor dimensions of the hexagonal prism-shaped inclusions in this sample can differ by as much as a factor of 4.

If we assume that the minor dimension of inclusion a in Figure 4A is 20 μm, and that the depth to its midplane is 20 μm below the polished surface, then the method of Ryan et al. (1991) would estimate an inclusion depth of 10 μm and an inclusion thickness of 20 μm. In contrast, the actual depth, as measured with the spindle stage, is 17.5 μm and the inclusion thickness is 5 μm. For this particular example, employing the method of Ryan et al. (1991) would result in a significant underestimation of the actual elemental concentration in the inclusion fluid. In general, the magnitude of the error will vary as a function of inclusion size and element atomic number but may vary by orders of magnitude for low-Z elements such as S and Cl. It is clear that more accurate determination of the size and depth of individual fluid inclusions will provide more reliable quantitative analysis with PIXE, especially in cases where the depth of an inclusion cannot be determined from the relative intensities of the ClK lines.

The destructive analysis of fluid inclusions (see Roedder, 1991) generally provides information on the relative amounts of components within an individual inclusion or group of inclusions. Inclusion volume estimates from spindle stage measurements may, in ideal cases, be combined with destructive analytical techniques such as laser ablation (e.g., Böhlke et al., 1989; Rankin et al., 1992) or the ion microprobe (Nambu and Sato, 1981; Diamond et al., 1990) to estimate the absolute concentrations of elements in single fluid inclusions.

Evaluation of decrepitation behavior

The most important features controlling the decrepitation behavior of fluid inclusions are the size and shape of the inclusions (Bodnar et al., 1989; Lacazette, 1991; Wanamaker et al., 1990; Wilkins et al., 1992). Thus, in order to predict when a given inclusion may decrepitate in the laboratory or to determine which inclusions may have decrepitated naturally as a result of uplift or burial, the size and shape must be known. Generally, workers use the diameter of inclusions as observed in two dimensions to approximate the size. However, as described above and shown in Figure 4, estimation of inclusion volume from dimensions observed in the plane of the microscope can lead to significant errors.

Conclusions

The modified spindle stage is a simple but powerful tool that can be applied to a variety of structural and mineralogical problems that require three-dimensional imaging of objects within a translucent medium. The use of the spindle stage eliminates many of the uncertainties in standard fluid inclusion petrography, which have long been the Achilles' heel of fluid inclusion studies. This new technique may also have potential in other studies requiring microscopic analysis of oriented features, such as fission track analyses, solid inclusion orientation analysis in porphyroblasts, and microstructural studies of rocks and synthetic materials.

The advantages of the modified spindle stage for fluid inclusion petrography and geometric analysis of three-dimensional features in minerals are summarized: (1) the spindle stage is simple to operate; (2) the spindle stage is inexpensive; (3) the spindle stage provides 360° rotation about the horizontal axis to permit measurement of all planar and linear features regardless of their orientation; (4) optical directions of the host crystal can be readily obtained and compared with inclusion plane orientations; (5) the spindle stage requires little or no sample preparation; single, unpolished grains or doubly polished sections are suitable.

Acknowledgments

F.D. Bloss is gratefully acknowledged for many helpful discussions. We would also like to thank K.L. Bartelmehs for a copy of the program EXCALBR II and B. Brockmyer for providing the quartz sample from Collegeville, Pennsylvania. D.M. Smith assisted with the construction of the oil immersion vessel. S.J. Reynolds and F. Robert are thanked for their helpful reviews.

A.J.A. acknowledges the receipt of a Natural Sciences and Engineering Research Council of Canada (NSERC) postdoctoral fellowship. This work was done while A.J.A. was on academic leave of absence from St. Francis Xavier University. This research was supported by NSF grant EAR-8657778 to R.J.B. Figure 6 is reprinted with the kind permission of John Wiley and Sons, Ltd.

References cited

Anderson, A.J., Clark, A.H., Ma, X.-P., Palmer, G.R., MacArthur, J.D., and Roedder, E. (1989) Proton-induced X-ray and gamma-ray emission analysis of unopened fluid inclusions. Economic Geology, 84, 924–939.

Bartelmehs, K.L., Bloss, F.D., Downs, R.T., and Birch, J.B. (1992) EXCALIBR II. Zeitschrift für Kristallographie, 199, 185–196.

Bloss, F.D. (1981) The spindle stage: Principles and practice, 340 p. Cambridge University Press, New York.

Bloss, F.D., and Gibbs, G.V. (1963) Cleavage in quartz. American Mineralogist, 48, 821–838.

Bodnar, R.J., Reynolds, T.J., and Kuehn, C.A. (1985) Fluid-inclusion systematics in epithermal systems. In Society of Economic Geologists Reviews in Economic Geology, 2, 73–97.

Bodnar, R.J., Binns, P.R., and Hall, D.L. (1989) Synthetic fluid inclusions. VI. Quantitative evaluation of the decrepitation behavior of fluid inclusions in quartz at one atmosphere confining pressure. Journal of Metamorphic Geology, 7, 229–242.

Böhlke, J.K., Kirschbaum, C., and Irwin, J. (1989) Simultaneous analysis of noble-gas isotopes and halogens in fluid inclusions in neutron-irradiated quartz veins by use of a laser-microprobe noble-gas spectrometer. U.S. Geological Survey Bulletin, 1980, 61–88.

Boiron, M.C., Essarraj, S., Sellier, E., Cathelineau, M., Lespinasse, M., and Poty, B. (1992) Identification of fluid inclusions in relation to their host microstructural domains in quartz by cathodoluminescence. Geochimica et Cosmochimica Acta, 56, 175–185.

Boullier, A.-M., and Robert, François (1991) Textures and orientations of fluid inclusion planes in gold-quartz veins in SE Abitibi Subprovince, Canada (abs.). ECROFI European current research on fluid inclusions XI symposium, Firenze, 10–12 April, 1991, 29–30.

——— (1992) Paleoseismic events recorded in Archean gold-quartz vein networks, Val d'Or, Abitibi, Quebec, Canada. Journal of Structural Geology, 14, 161–179.

Brantley, S.L., Evans, B., Hickman, S.H., and Crerar, D.A. (1990) Healing of microcracks in quartz: Implications for fluid flow. Geology, 18, 136–139.

Diamond, L.W., Marshall, D.D., Jackman, J.A., and Skippen, G.B. (1990) Elemental analysis of individual fluid inclusions in minerals by secondary ion mass spectrometry (SIMS): Application to cation ratios of fluid inclusions in an Archaean mesothermal gold-quartz vein. Geochimica et Cosmochimica Acta, 54, 545–552.

Frantz, J.D., Mao, H.K., Zhang, Y.G., Wu, Y., Thompson, A.C., Underwood, J.H., Giauque, R.D., Jones, K.W., and Rivers, M.L. (1988) Analysis of fluid inclusions by X-ray fluorescence using synchrotron radiation. Chemical Geology, 69, 235–244.

Frondel, C. (1962) The system of mineralogy. Vol. 3. Silica minerals (7th edition), 334 p. Wiley, New York.

Kesler, S.E. (1990) Nature and composition of mineralizing solutions. In F. Robert, P.A. Sheahan, and S.B. Green, Eds., NUNA conference on greenstone gold and crustal evolution, Val d'Or, May, 1990, p. 86–90. Geological Association of Canada, St. John's, Newfoundland.

Lacazette, A. (1991) Reply on "Application of linear elastic fracture mechanics to the quantitative evaluation of fluid-inclusion decrepitation." Geology, 19, 663–664.

——— (1992) Fluid inclusions as paleostressmeters with examples from the fold-thrust belt of central Pennsylvania (abs.). PACROFI IV: Pan-American Conference on research on fluid inclusions, Lake Arrowhead, California, 21–25 May, 1992, 48.

Laubach, S.E. (1989) Paleostress directions from the preferred orientation of closed microfractures (fluid inclusion planes) in sandstone, East Texas basin, U.S.A. Journal of Structural Geology, 11, 603–611.

Lespinasse, M., and Pecher, A. (1986) Microfracturing and regional stress field: A study of the preferred orientation of fluid inclusion planes in a granite from the Massif Central, France. Journal of Structural Geology, 8, 169–180.

Lespinasse, M., Cathelineau, M., and Poty, B. (1992) Time-space reconstruction of fluid migration in relation with rock deformation: The use of fluid inclusion planes (abs.). PACROFI IV: Pan-American Conference on research on fluid inclusions, Lake Arrowhead, California, 21–25 May, 1992, 52.

Nambu, M., and Sato, T. (1981) The analysis of fluid inclusions in the microgram range with an ion microanalyzer. Bulletin de Mineralogie, 104, 827–833.

Nicolas, A., and Poirier, J.P. (1976) Crystalline plasticity and solid state flow in metamorphic rocks, 444 p. Wiley, London.

Petford, N., and Miller, J.A. (1992) Three-dimensional imaging of fission tracks using confocal scanning laser microscopy. American Mineralogist, 77, 529–533.

Rankin, A.H., Ramsey, M.H., Coles, B., Van Langevelde, F., and Thomas, C.R. (1992) The composition of hypersaline, iron-rich granitic fluids based on laser-ICP and Synchrotron-XRF microprobe analysis of individual fluid inclusions in topaz, Mole granite, eastern Australia. Geochimica et Cosmochimica Acta, 56, 67–79.

Ren, X., Kowallis, B.J., and Best, M.G. (1989) Paleostress history of the Basin and Range province in western Utah and eastern Nevada from healed microfracture orientations in granites. Geology, 17, 487–490.

Roedder, E. (1984) Fluid inclusions. Mineralogical Society of America Reviews in Mineralogy, 12, 644 p.

——— (1991) Fluid inclusion analysis: Prologue and epilogue. Geochimica et Cosmochimica Acta, 54, 495–507.

Ryan, C.G., Cousens, D.R., Heinrich, C.A., Griffin, W.L., Sie, S.H., and Mernagh, T.P. (1991) Quantitative PIXE microanalysis of fluid inclusions based on a layered yield model. Nuclear Instruments and Methods in Physics Research, B54, 292–297.

Smith, D.L., and Evans, B. (1984) Diffusional crack healing in quartz. Journal of Geophysical Research, 89, 4125–4135.

Tuttle, O.F. (1949) Structural petrology of planes of liquid inclusions. Journal of Geology, 57, 331–356.

Wanamaker, B.J., Wong, T.F., and Evans, B. (1990) Decrepitation and crack-healing of fluid inclusions in San Carlos olivine. Journal of Geophysical Research, 95, 15623–15641.

Wilcox, R.E. (1959) Use of spindle stage for determining refractive indices of crystal fragments. American Mineralogist, 44, 1272–1293.

Wilkins, R.W.T., Hladky, G., Gratier, J.-P., and Jenatton, L. (1992) Some relationships between cracks and fluid inclusions (abs.). PACROFI IV: Pan-American Conference on research on fluid inclusions, Lake Arrowhead, California, 21–25 May, 1992, 89.

Manuscript received September 14, 1992
Manuscript accepted January 9, 1993